ACS APPLIED MATERIALS & INTERFACES

Letter

www.acsami.org

Ca^{2+}-Controlled Assembly for Visualized Detection of Conformation Changes of Calmodulin

Hongbo Yuan, Chengfen Xing,* Hailong An, Ruimin Niu, Ruihua Li, Wenmin Yan, and Yong Zhan*

Key Laboratory of Hebei Province for Molecular Biophysics, Institute of Biophysics, Hebei University of Technology, Tianjin 300401, P. R. China

Supporting Information

ABSTRACT: A new strategy has been designed for visualized detection of the conformation changes of calmodulin bound to target peptide (CaM-M13) based on the conformation sensitive property of a water-soluble conjugated polythiophene derivative (PMNT) and the electrostatic interactions of PMNT/CaM-M13. Interestingly, the direct visualized PMNT color changes under UV irradiation and the turbidity changes of samples in aqueous medium can be applied to detect the conformation changes as well as the controllable assembly of PMNT/CaM-M13 with Ca^{2+} in aqueous medium. Because of the specific binding of Ca^{2+}, the assembly of PMNT/CaM-M13 can be applied to sense calcium as well.

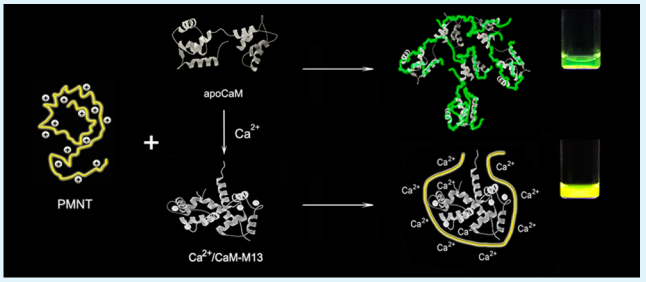

KEYWORDS: *assembly, calcium, CaM-M13, conformation changes, conjugated polythiophene*

Calmodulin (CaM) functions as a calcium sensor in cells, mediating a variety of intracellular signaling transductions by binding to calcium.[1] The extended conformation of calcium free form of CaM converts to a compact structure upon binding with target protein in the presence of calcium.[2] The C terminus of CaM has been bound to the target peptide of M13, the 577 to 602 residues of skeletal myosin light-chain kinase, leading to the formation of the hybrid protein of CaM-M13.[3] The extended dumbbell-like conformation of calcium free form (apoCaM-M13) converts to a compact globular structure upon binding with Ca^{2+} (Ca^{2+}/CaM-M13).[2−5] Such a conformation change is a very important biomolecular process, forming one part in Ca^{2+} mediated intracellular signaling transductions.[6] The most conventional techniques to determine the conformations of protein include X-ray crystallography,[7] NMR spectroscopy,[2] and single-pair fluorescence resonance energy transfer.[8] However, these methods require expensive instruments, complicated procedures, and veteran experimenter, which limits their applications. Therefore, a new, simple, highly sensitive and selective approach to the detection of the conformation change process of CaM-M13 is urgently needed.

Water-soluble conjugated polymers (WCP) are well-known for their light-harvesting properties and signal amplifications by coordinating the action of a large number of absorbing units.[9−11] WCP have been used for sensitive detection of biological macromolecules and fluorescence imaging, offering remarkable advantages in contrast to small molecule probes.[12−18] The optical properties of conjugated polythiophene have been reported to be highly sensitive to conformational variations of its conjugated backbone.[19−22] For example, Nilsson and Inganäs have introduced conjugated polythiophene as a sensitive optical conformation probe to detect amyloid fibrils and the conformational changes of calmodulin.[15,23−26] Inspired by these observations, we describe here a new simple, label-free, highly sensitive visual detection for conformation change of CaM-M13 and present a strategy to control the formation of assemblies of CaM-M13 with PMNT in aqueous medium based on the conformational flexibility of PMNT.

As illustrated in Scheme 1, we employed a water-soluble, positively charged conjugated polythiophene, poly(3-(3′-*N*,*N*,*N*-triethylamino-1′-propyloxy)-4-methyl-2,5-thiophene hydrochloride) (PMNT) to detect the conformation changes of CaM-M13. The anionic CaM-M13 with many negatively charged amino acid residues in the four EF-hands of opposing globular domains and the central linker region can form micrometer-sized supramolecular complexes with the cationic PMNT by intense electrostatic interactions, in which PMNT backbone coiled around CaM and transform from a random-coil conformation to a more nonplanar and less conjugated conformation, exhibiting relatively blue-shifted absorption and emission wavelength. However, the blue-shifted values decrease gradually with the addition of Ca^{2+} ions due to the transformation of extended form of apoCaM-M13 to compact form of Ca^{2+}/CaM-M13, which induces the PMNT to return to its random-coil conformation. Moreover, the negative charge density of Ca^{2+}/CaM-M13 becomes lower in contrast to that of apoCaM-M13, and the free Ca^{2+} ions in solution make the negative charge density on surface of CaM-M13 decrease.

Received: July 18, 2014
Accepted: August 25, 2014
Published: August 25, 2014

   dx.doi.org/10.1021/am504729d | *ACS Appl. Mater. Interfaces* 2014, 6, 14790−14794

Scheme 1. (a) Schematic Representation of the Detection of Conformation Changes of CaM-M13 and Ca^{2+} Controllable Assembly of PMNT/CaM-M13; (b) Chemical Structure of the PMNT

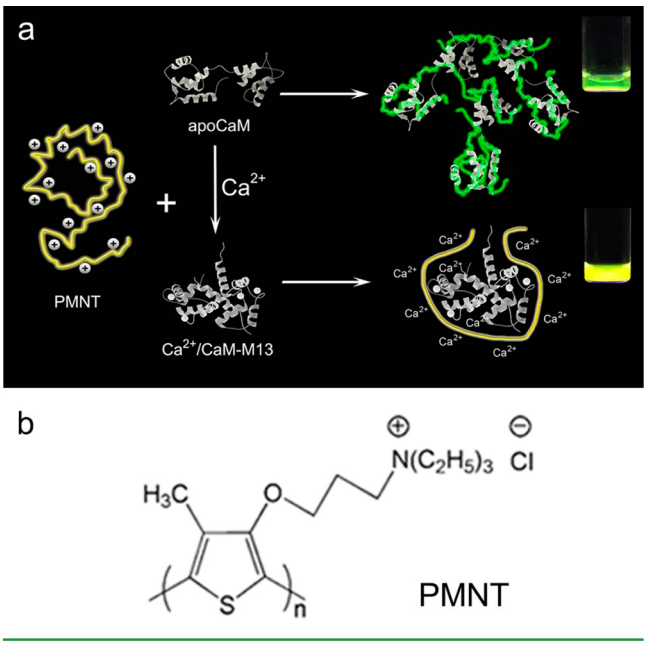

Therefore, Ca^{2+} ions can induce micrometer-sized supramolecular complexes into well-separate nanoparticles in aqueous medium. Furthermore, the conformational changes of CaM-M13 and the Ca^{2+} controllable assembly of CaM-M13 with PMNT can be visualized directly by "naked-eye" in view of the turbidity changes of samples in aqueous medium and PMNT color changes under UV irradiation.

The PMNT shows an absorption maximum at 410 nm, relating to the $\pi-\pi^*$ transition of the conjugated polythiophenes.[27] The molecular weights of the cationic polythiophene showed that the polymers contain 20−40 thiophene repeat units in the backbone,[27] indicating the intense interpolyelectrolyte interactions between PMNT and CaM-M13. The PMNT emits yellow fluorescence in Tris-HCl buffer with UV light irradiation and exhibits emission spectra with a maximum at 523 nm, corresponding to a flexible and random-coil conformation of the polythiophenes backbone.[19,28,29] Upon addition of CaM-M13 ([PMNT] = 25.0 μM in repeat units (RUs), [CaM-M13] = 1.4 μM), the absorption maximum of PMNT was blue-shifted by 13 nm (Figure 1a), indicating a transformation from a random-coil conformation to a more nonplanar and less conjugated conformation and the formation of the electrostatic complexes of PMNT with CaM-M13. The blue-shifted value ($\Delta\lambda$) of absorption maximum of PMNT with successive addition of CaM-M13 was also examined. As shown in Figure 1b, it exhibits the increase of $\Delta\lambda$ with adding CaM-M13 and the detection limit can be lowered to 6.16 pmol. However, the $\Delta\lambda$ decrease gradually with the addition of Ca^{2+} ions (Figure 1d). When the concentration of Ca^{2+} ions increase to 5.0 mM, the absorption maximum of PMNT return to 410 nm (Figure 1c), the same to that of free PMNT in aqueous solution, implying the fact that the PMNT backbone returned to the random-coil conformation of the PMNT alone. Furthermore, the effect of the concentration of Tris-HCl buffer to the $\Delta\lambda$ was also checked (see Figure S1 in the Supporting Information), and the UV−vis spectra and fluorescence emission show about 20 nm changes between PMNT and PMNT/CaM-M13 with 100 mM of Tris-HCl buffer, maximizing the difference of PMNT/CaM-M13 with and without Ca^{2+}. Interestingly, the turbidity changes can be observed by absorption spectra (see Figure S3 in the Supporting Information) as well as by the naked eye during this

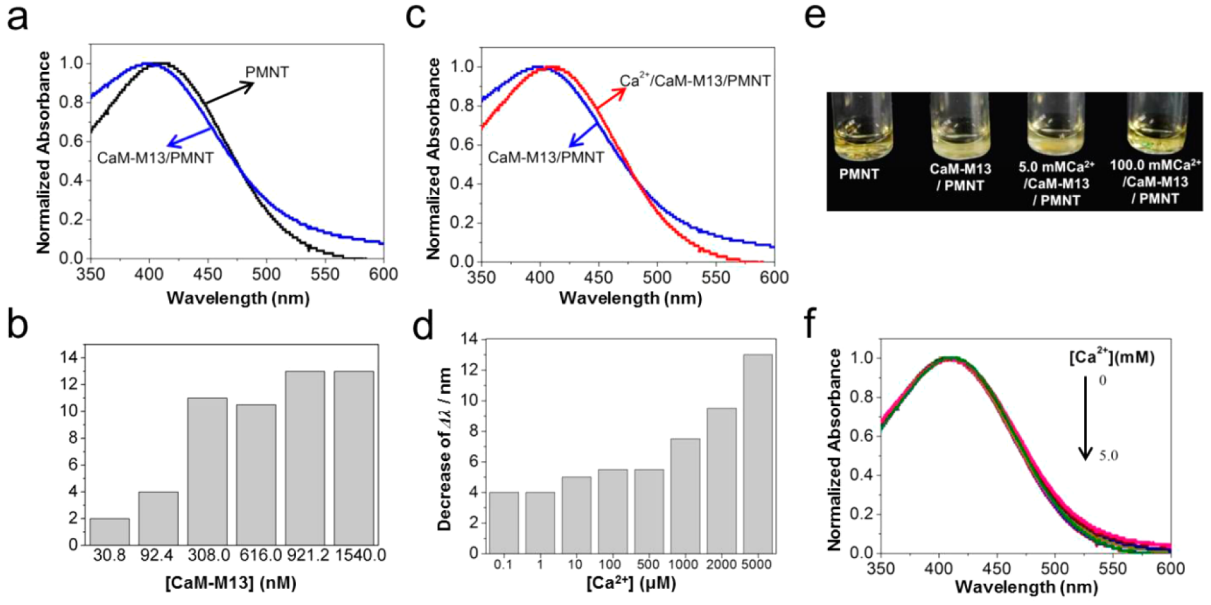

Figure 1. (a) The UV−vis spectra of PMNT in the absence and presence of CaM-M13. (b) Blue-shifted value ($\Delta\lambda$) of absorption maximum of PMNT with successive addition of CaM-M13. (c) UV−vis spectra of CaM-M13/PMNT with and without Ca^{2+} (5.0 mM). (d) The decrease of $\Delta\lambda$ of absorption maximum of CaM-M13/PMNT as a function of Ca^{2+} concentrations. (e) Photographs of PMNT, CaM-M13/PMNT, 5.0 mM Ca^{2+}/CaM-M13/PMNT, and 100.0 mM Ca^{2+}/CaM-M13/PMNT. [PMNT] = 150.0 μM in repeat units (RUs), [CaM-M13] = 8.4 μM. (f) UV−vis spectra of PMNT with successive addition of Ca^{2+}. Measurements were performed in Tris-HCl buffer solution (20.0 mM, pH 7.4).

dx.doi.org/10.1021/am504729d | ACS Appl. Mater. Interfaces 2014, 6, 14790−14794

conformational changing process. As shown in Figure 1e, it shows the changes from clear to turbid upon forming complexes of CaM-M13/PMNT, and the complexes reconvert to clear solution along with the addition of Ca^{2+} ions, implying that the anionic CaM-M13 can form supramolecular complexes with the cationic PMNT by electrostatic interactions and Ca^{2+} ions separate the complexes in aqueous medium. The control experiment shows that Ca^{2+} ions cannot alter the absorption spectra of PMNT when adding Ca^{2+} ions successively into solution of PMNT (Figure 1f). These results demonstrate a simple, convenient, and visualized detection of the conformation changes of CaM-M13 and the formation of electrostatic assemblies of CaM-M13/PMNT.

Figure 2 suggests that the fluorescence emission spectra can be applied to probe the conformational changes of CaM-M13

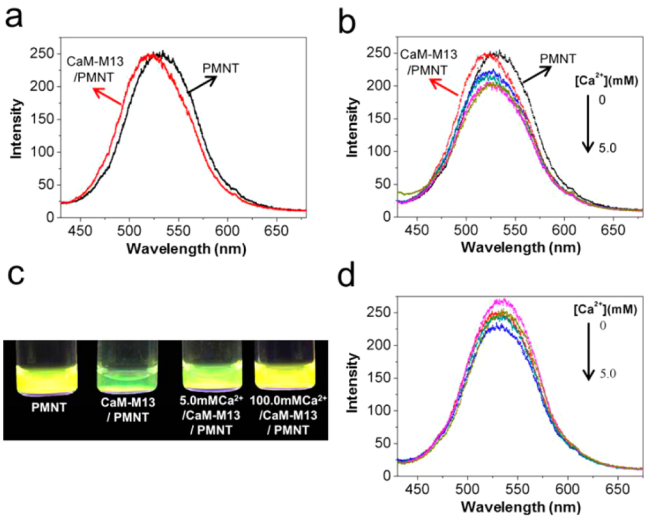

Figure 2. (a) Emission spectra of PMNT, CaM-M13/PMNT. (b) Emission spectra of CaM-M13/PMNT as a function of Ca^{2+} concentrations. (c) Fluorescence images of PMNT, CaM-M13/PMNT, 5.0 mM Ca^{2+}/CaM-M13/PMNT, and 100 mM Ca^{2+}/CaM-M13/PMNT under UV light (λ_{max} = 365 nm). [PMNT] = 150.0 μM in RUs, [CaM-M13] = 8.4 μM. (d) Emission spectra of PMNT with successive addition of Ca^{2+}. Measurements were performed in Tris-HCl buffer solution (20.0 mM, pH 7.4). The excitation wavelength is 410 nm.

as well. Upon the addition of CaM-M13, the emission maximum was blue-shifted by 11 nm (Figure 2a), and the blue-shifted value decrease gradually with the addition of Ca^{2+} ions ([Ca^{2+}] = 0−5.0 mM) (Figure 2b). When the concentration of Ca^{2+} ions increase to 5.0 mM, the emission spectra of PMNT return to the same with that of free PMNT in aqueous solution. The fluorescence measurements indicate that the PMNT exhibits relatively blue-shifted emission wavelength as a result of the less conjugated and more nonplanar conformation in comparison to PMNT itself in CaM-M13/PMNT complexes, and then reconvert to the random-coil conformation induced by Ca^{2+} ions. Fluorescence images of PMNT, CaM-M13/PMNT, and Ca^{2+}/CaM-M13/PMNT under UV light presented a noticeable color changes from yellow to green and then return to yellow (Figure 2c). From the emission spectra, fluorescence images and minor interference to the emission of PMNT from Ca^{2+} ions (Figure 2d), it offers a versatile methodology without any expensive equipment and sophisticated procedures to probe the CaM-M13 conformational transition. To determine the optimum working pH condition, the blue-shifted value ($\Delta\lambda$) of absorption maximum (see Figure S4 in the Supporting Information) and emission maximum (see Figure S5 in the Supporting Information) for CaM-M13/PMNT and Ca^{2+}/CaM-M13/PMNT at various pH were measured, indicating that the system could satisfy with the physiological pH range.

We conducted the control absorbance and emission measurements for solutions of PMNT containing natural calmodulin (CaM) without M13 in the absence and presence of Ca^{2+}, showing a slight shift as well as that for albumin from bovine serum (BSA), lysozyme (LZM), and streptavidin (SA), implying that binding to the target peptide of M13 causes the transition from the extended dumbbell-like conformation of calcium free form to a compact globular structure in the presence of Ca^{2+} and then lead to the conformational change of PMNT (Table 1). It is noteworthy that the assembly of

Table 1. Absorption Maximum, Emission Maximum, and the Shifted Value ($\Delta\lambda$) for Solutions of PMNT Containing Different Kinds of Proteins (CaM-M13, CaM, BSA, LZM, SA) in the Absence and Presence of Ca^{2+}

	absorption max (nm)			emission max (nm)		
	protein/ PMNT	Ca^{2+}/ protein/ PMNT	$\Delta\lambda$	protein/ PMNT	Ca^{2+}/ protein/ PMNT	$\Delta\lambda$
CaM-M13	396	408	12	511	522	11
CaM	399	397	−2	511	509	−2
BSA	394	396	2	516	516	0
LZM	410	410	0	522	522	0
SA	408	410	2	518	518	0

PMNT/CaM-M13 can also be used to sense Ca^{2+} ions with high selectivity because of the specific binding of Ca^{2+} (see Figure S6 in the Supporting Information). The decrease in blue-shifted value ($\Delta\lambda$) of absorption maximum of PMNT in Ca^{2+}/CaM-M13/PMNT versus incubation time of CaM-M13/Ca^{2+} in Tris-HCl buffer was also investigated, indicating that PMNT can be used to detect the process of conformation changes (see Figure S7 in the Supporting Information).

To investigate the controllable supramolecular assemblies by calcium in aqueous medium, we performed the dynamic light scattering (DLS) measurements in Tris-HCl buffer (20 mM, pH 7.4). As shown in Figure 3, the average hydrodynamic radius of CaM-M13/PMNT was about 1 μm, which was much

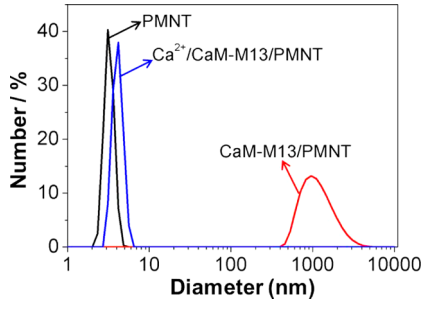

Figure 3. Dynamic light scattering analysis of PMNT, CaM-M13/PMNT, and Ca^{2+}/CaM-M13/PMNT in Tris-HCl buffer (20.0 mM). [PMNT] = 30.0 μM in repeat units (RUs), [CaM-M13] = 1.4 μM, [Ca^{2+}] = 100.0 mM.

dx.doi.org/10.1021/am504729d | ACS Appl. Mater. Interfaces 2014, 6, 14790−14794

larger than that of PMNT and CaM-M13 themself, indicating the formation of larger assembly or aggregation upon addition of CaM-M13 in Tris-HCl buffer and thus the turbid suspension was observed. However, upon the addition of Ca^{2+} ions in aqueous medium, the micrometer-sized supramolecular complexes were disassembled to well-separate nanoparticles with the average hydrodynamic radius of 5 nm, which is close to that of PMNT itself. Furthermore, ζ potentials of CaM-M13 and CaM-M13/PMNT complex with and without Ca^{2+} ions have also been examined in Tris-HCl buffer (Table 2). For CaM-M13/PMNT complex, ζ potential became less cationic than that of PMNT itself, confirming the electrostatic interactions between PMNT and CaM-M13. For CaM-M13, its ζ potentials data demonstrated that the surface charges became less when binding with Ca^{2+} ions, from −13.0 to −3.1 mV, leading to the weak interactions with PMNT and then disassembly of supramolecular complexes of CaM-M13/PMNT. Considering the DLS and ζ potential measurements, it is proposed that the intense electrostatic interaction between the PMNT and apoCaM-M13 makes the formation of micrometer-sized supramolecular assemblies of CaM-M13/PMNT. The CaM-M13 bind with Ca^{2+} in four EF-hands domains and then convert to a compact structure of Ca^{2+}/CaM-M13 when adding Ca^{2+}, and the negative charge density of Ca^{2+}/CaM-M13 becomes lower in contrast to that in apoCaM-M13. Therefore, PMNT return to the random-coil conformation and the assemblies of CaM-M13/PMNT disassemble in aqueous media.

Table 2. ζ Potential of PMNT, CaM-M13, Ca^{2+}/CaM-M13, CaM-M13/PMN, and Ca^{2+}/CaM-M13/PMNT in Tris-HCl Buffer (20.0 mM, pH 7.4)

	ζ potential (mV)
PMNT	21.9
CaM-M13	−13.0
Ca^{2+}/CaM-M13	−3.1
CaM-M13/PMNT	7.28
Ca^{2+}/CaM-M13/PMNT	14.9

In conclusion, we have developed a straightforward, simple, label-free, and highly sensitive visualized detection for the conformation changes of calmodulin bound to target peptide and calcium controllable assembly in aqueous medium based on the conformational flexibility of PMNT. The new electrostatic complex of PMNT/CaM-M13 has several significant characteristics. First, PMNT/CaM-M13 complex can be obtained without covalent linkage of chemical ligands and fluorescent labels, which reduces complicated synthesis procedures. Second, Ca^{2+} ions induce the micrometer-sized supramolecular complexes of PMNT/CaM-M13 into well-separated nanoparticles in aqueous medium. Third, the transition of apoCaM-M13 to Ca^{2+}/CaM-M13 and the Ca^{2+} controllable assembly of CaM-M13 with PMNT were directly visualized with naked-eye by the turbidity changes of samples in aqueous medium and the fluorescence color changes. Last but not the least, the assembly of PMNT/CaM-M13 can also be applied as a platform for Ca^{2+} detection. This strategy is potential to detect conformation changes induced by biospecific interactions and construct controllable hybrid materials.

■ ASSOCIATED CONTENT

Ⓢ Supporting Information

Experimental section and supplementary figures. This material is available free of charge via the Internet at http://pubs.acs.org.

■ AUTHOR INFORMATION

Corresponding Authors

*E-mail: xingc@hebut.edu.cn.
*E-mail: zhan_yong2014@163.com.

Author Contributions

C.X. and Y.Z. designed experiments and organized the manuscript; H.Y. performed experimental part and analyzed data; R.N., W.Y. and R.L. performed experimental part; H.A. analyzed data.

Notes

The authors declare no competing financial interest.

■ ACKNOWLEDGMENTS

We are grateful for the financial support of the Scientific Innovation Grant for Excellent Young Scientists of Hebei University of Technology (2013003) and the Key Discipline of Hebei Province for Biophysics. We acknowledge Prof. Libing Liu (Institute of Chemistry, Chinese Academy of Sciences) for valuable suggestions and some experimental performance.

■ REFERENCES

(1) Chin, D.; Means, A. R. Calmodulin: A Prototypical Calcium Sensor. *Trends Cell Biol.* **2000**, *10*, 322−328.

(2) Ikura, M.; Clore, G. M.; Gronenborn, A. M.; Zhu, G.; Klee, C. B.; Bax, A. Solution Structure of a Calmodulin-Target Peptide Complex by Multidimensional NMR. *Science* **1992**, *256*, 632−638.

(3) Miyawaki, A.; Llopis, J.; Heim, R.; McCaffery, J. M.; Adams, J. A.; Ikura, M.; Tsien, R. Y. Fluorescent Indicators for Ca^{2+} Based on Green Fluorescent Proteins and Calmodulin. *Nature* **1997**, *388*, 882−887.

(4) Osawa, M.; Tokumitsu, H.; Swindells, M. B.; Kurihara, H.; Orita, M.; Shibanuma, T.; Furuya, T.; Ikura, M. A Novel Target Recognition Revealed by Calmodulin in Complex with Ca^{2+}-Calmodulin-Dependent Kinase Kinase. *Nat. Struct. Biol.* **1999**, *6*, 819−824.

(5) Finn, B. E.; Forsen, S. The Evolving Model of Calmodulin Structure, Function and Activation. *Structure* **1995**, *3*, 7−11.

(6) Zhang, M.; Abrams, C.; Wang, L.; Gizzi, A.; He, L.; Lin, R.; Chen, Y.; Loll, P. J.; Pascal, J. M.; Zhang, J. F. Structural Basis for Calmodulin as a Dynamic Calcium Sensor. *Structure* **2012**, *20*, 911−923.

(7) Babu, Y. S.; Bugg, C. E.; Cook, W. J. Structure of Calmodulin Refined at 2.2 A Resolution. *J. Mol. Biol.* **1988**, *204*, 191−204.

(8) Slaughter, B. D.; Unruh, J. R.; Allen, M. W.; Bieber Urbauer, R. J.; Johnson, C. K. Conformational Substates of Calmodulin Revealed by Single-Pair Fluorescence Resonance Energy Transfer: Influence of Solution Conditions and Oxidative Modification. *Biochemistry* **2005**, *44*, 3694−3707.

(9) Swager, T. M. The Molecular Wire Approach to Sensory Signal Amplification. *Acc. Chem. Res.* **1998**, *31*, 201−207.

(10) Leclerc, M. Optical and Electrochemical Transducers Based on Functionalized Conjugated Polymers. *Adv. Mater.* **1999**, *11*, 1491−1498.

(11) Feng, L. H.; Zhu, C. L.; Yuan, H. X.; Liu, L. B.; Lv, F. T.; Wang, S. Conjugated Polymer Nanoparticles: Preparation, Properties, Functionalization and Biological Applications. *Chem. Soc. Rev.* **2013**, *42*, 6620−6633.

(12) Wang, F.; Liu, Z.; Wang, B.; Feng, L.; Liu, L.; Lv, F.; Wang, Y.; Wang, S. Multi-Colored Fibers by Self-Assembly of DNA, Histone Proteins, and Cationic Conjugated Polymers. *Angew. Chem., Int. Ed.* **2014**, *53*, 424−428.

(13) Feng, L.; Liu, L.; Lv, F.; Bazan, G. C.; Wang, S. Preparation and Biofunctionalization of Multicolor Conjugated Polymer Nanoparticles

for Imaging and Detection of Tumor Cells. *Adv. Mater.* **2014**, *26*, 3926−3930.
(14) Usmani, S. M.; Zirafi, O.; Muller, J. A.; Sandi-Monroy, N. L.; Yadav, J. K.; Meier, C.; Weil, T.; Roan, N. R.; Greene, W. C.; Walther, P.; Nilsson, K. P. R.; Hammarstrom, P.; Wetzel, R.; Pilcher, C. D.; Gagsteiger, F.; Faendrich, M.; Kirchhoff, F.; Munch, J. Direct Visualization of HIV-Enhancing Endogenous Amyloid Fibrils in Human Semen. *Nat. Commun.* **2014**, *5*, 3508.
(15) Nilsson, K. P. R.; Hammarström, P. In *Conjugated Polyelectrolytes: Fundamentals and Applications*; Liu, B., Bazan, G. C., Eds.; Wiley−VCH: Weinheim, Germany, 2013; Chapter 9, pp 295−314.
(16) Feng, X.; Liu, L.; Wang, S.; Zhu, D. Water-Soluble Fluorescent Conjugated Polymers and Their Interactions with Biomacromolecules for Sensitive Biosensors. *Chem. Soc. Rev.* **2010**, *39*, 2411−2419.
(17) Lan, M.; Wu, J.; Liu, W.; Zhang, W.; Ge, J.; Zhang, H.; Sun, J.; Zhao, W.; Wang, P. Copolythiophene-Derived Colorimetric and Fluorometric Sensor for Visually Supersensitive Determination of Lipopolysaccharide. *J. Am. Chem. Soc.* **2012**, *134*, 6685−6694.
(18) Lan, M.; Liu, W.; Wang, Y.; Ge, J.; Wu, J.; Zhang, H.; Chen, J.; Zhang, W.; Wang, P. Copolythiophene-Derived Colorimetric and Fluorometric Sensor for Lysophosphatidic Acid Based on Multipoint Interactions. *ACS Appl. Mater. Interfaces* **2013**, *5*, 2283−2288.
(19) Tang, Y. L.; He, F.; Yu, M. H.; Feng, F. D.; An, L. L.; Sun, H.; Wang, S.; Li, Y. L.; Zhu, D. B. A Reversible and Highly Selective Fluorescent Sensor for Mercury(II) Using Poly (thiophene)s that Contain Thymine Moieties. *Macromol. Rapid Commun.* **2006**, *27*, 389−392.
(20) Pu, F.; Hu, D.; Ren, J.; Wang, S.; Qu, X. Universal Platform for Sensitive and Label-Free Nuclease Assay Based on Conjugated Polymer and DNA/Intercalating Dye Complex. *Langmuir* **2009**, *26*, 4540−4545.
(21) Ho, H. A.; Najari, A.; Leclerc, M. Optical Detection of DNA and Proteins with Cationic Polythiophenes. *Acc. Chem. Res.* **2008**, *41*, 168−178.
(22) Charlebois, I.; Gravel, C.; Arrad, N.; Boissinot, M.; Bergeron, M. G.; Leclerc, M. Impact of DNA Sequence and Oligonucleotide Length on a Polythiophene-Based Fluorescent DNA Biosensor. *Macromol. Biosci.* **2013**, *13*, 717−722.
(23) Nilsson, K. P. R.; Hammarstrom, P.; Ahlgren, F.; Herland, A.; Schnell, E. A.; Lindgren, M.; Westermark, G. T.; Inganas, O. Conjugated Polyelectrolytes-Conformation-Sensitive Optical Probes for Staining and Characterization of Amyloid Deposits. *Chembiochem* **2006**, *7*, 1096−1104.
(24) Herland, A.; Nilsson, K. P.; Olsson, J. D.; Hammarstrom, P.; Konradsson, P.; Inganas, O. Synthesis of a Regioregular Zwitterionic Conjugated Oligoelectrolyte, Usable as an Optical Probe for Detection of Amyloid Fibril Formation at Acidic pH. *J. Am. Chem. Soc.* **2005**, *127*, 2317−2323.
(25) Arja, K.; Sjolander, D.; Aslund, A.; Prokop, S.; Heppner, F. L.; Konradsson, P.; Lindgren, M.; Hammarstrom, P.; Aslund, K. O. A.; Nilsson, K. P. R. Enhanced Fluorescent Assignment of Protein Aggregates by an Oligothiophene-Porphyrin-Based Amyloid Ligand. *Macromol. Rapid Commun.* **2013**, *34*, 723−730.
(26) Aslund, A.; Sigurdson, C. J.; Klingstedt, T.; Grathwohl, S.; Bolmont, T.; Dickstein, D. L.; Glimsdal, E.; Prokop, S.; Lindgren, M.; Konradsson, P.; Holtzman, D. M.; Hof, P. R.; Heppner, F. L.; Gandy, S.; Jucker, M.; Aguzzi, A.; Hammarstrom, P.; Nilsson, K. P. Novel Pentameric Thiophene Derivatives For in Vitro and in Vivo Optical Imaging of a Plethora of Protein Aggregates in Cerebral Amyloidoses. *ACS Chem. Biol.* **2009**, *4*, 673−684.
(27) Tang, Y.; Feng, F.; He, F.; Wang, S.; Li, Y.; Zhu, D. Direct Visualization of Enzymatic Cleavage and Oxidative Damage by Hydroxyl Radicals of Single-Stranded DNA with a Cationic Polythiophene Derivative. *J. Am. Chem. Soc.* **2006**, *128*, 14972−14976.
(28) Ho, H. A.; Boissinot, M.; Bergeron, M. G.; Corbeil, G.; Dore, K.; Boudreau, D.; Leclerc, M. Colorimetric and Fluorometric Detection of Nucleic Acids Using Cationic Polythiophene Derivatives. *Angew. Chem., Int. Ed.* **2002**, *41*, 1548−1551.
(29) Liu, X. F.; Tang, Y. L.; Wang, L. H.; Zhang, J.; Song, S. P.; Fan, C. H.; Wang, S. Optical Detection of Mercury(II) in Aqueous Solutions by Using Conjugated Polymers and Label-free Oligonucleotides. *Adv. Mater.* **2007**, *19*, 1662−1662.